Evidence for structurally different attached states of myosin cross-bridges on actin during contraction of fish muscle

Jeffrey J. Harford and John M. Squire
Biophysics Section, Blackett Laboratory, Imperial College, London SW7 2BZ United Kingdom

ABSTRACT Using data from fast time-resolved x-ray diffraction experiments on the synchrotrons at Daresbury and (Deutsches Elektronen Synchrotron [DESY]), it is shown that during contraction of fish muscle there are at least two distinct configurations of myosin cross-bridges on actin, that they appear to have different tension producing properties and that they probably differ in the axial tilt of the cross-bridges on actin. Evidence is presented for newly observed myosin-based layer lines in patterns from active fish muscle, together with intensity changes of the actin layer lines. On the equator, the 110 reflection changes much faster (time for 50% change $t_{1/2} = 21 \pm 4$ ms after activation) than the 100 reflection ($t_{1/2} = 35 \pm 8$ ms) and tension ($t_{1/2} = 41 \pm 3$ ms) during the rising phase of tetanic contractions. These and higher order reflections have been used to show the time course of mass attachment at actin during this rising phase. Mass arrival ($t_{1/2} = 25$ ms) precedes tension by ~15 ms. Analysis has been carried out to evaluate the effects of changes in sarcomere length during the tetanus. It is shown that any such effects are very small. Difference "equatorial" electron density maps between active muscle at a time when mass arrival at actin is just complete, but the tension is still rising, and at a later time well into the tension plateau, show that the structural difference between the lower and higher force states corresponds to mass movement consistent with axial swinging of heads from a nonstereospecific actin attached state (low force) to a more stereospecific (high force) state.

INTRODUCTION

After the publication of the sliding filament model of muscular contraction, attempts to define the molecular mechanism giving rise to filament motion have concentrated on the "swinging crossbridge" model (Reedy et al., 1965; Huxley, 1969; Huxley and Simmons, 1971). Myosin cross-bridges projecting from the myosin filament surface are postulated to attach to, rotate on and then detach from the neighboring actin filaments in a repetitive cyclic process. Although a considerable volume of biochemical and mechanical data exists in support of such a model (Huxley and Simmons, 1971; Huxley, 1973; Eisenberg and Hill, 1978; Squire, 1981; see reviews in Squire, 1990) it has proved to be extremely difficult to demonstrate this mechanism conclusively by structural methods. In particular, no change in attachment configuration of myosin cross-bridges on actin has ever been demonstrated directly in structural studies of active muscle. In addition, it has been a puzzle why, if significant actin binding occurs during force production, there is not a major intensification of the x-ray layer-line pattern from the actin filaments; intensification similar to that which occurs, for example, in patterns from muscles in the rigor state where virtually all of the myosin heads are linked to actin in a stereospecific manner. (By stereospecific we mean that the actin-binding region of the myosin head has a characteristic three-dimensional geometry relative to the actin monomer to which it binds). In this paper we provide structural evidence for at least two distinct states of cross-bridge attachment to actin during muscle contraction, and we show that these states appear to have different tension producing properties and to involve different axial tilts of the myosin heads.

Previous biochemical studies of actomyosin solutions, and mechanical and structural studies of muscle fibers, all under nonphysiological conditions, have demonstrated the existence of two equilibrium states involving myosin head attachment to actin. One is the well-known rigor state produced in the absence of ATP (Huxley, 1968; Miller and Tregear, 1972; Holmes et al., 1980). This is a state of stereospecific attachment of the myosin heads to actin in which the axis of the myosin head is tilted and slewed relative to the actin filament long axis (Miller and Tregear, 1972; Holmes et al., 1980; Squire, 1981). In this case the attached heads follow the symmetry of the actin helix and label actin with their center of mass at a relatively small radius from the actin filament axis. The other state is one induced by low ionic strength relaxing solutions (containing Mg-ATP but no Ca^{2+} ions), at nonphysiological temperatures (e.g., 5 to 20°C for rabbit psoas muscle fibers). Here, stiffness measurements (Brenner et al., 1982), solution studies (Eisenberg and Hill, 1985) and x-ray diffraction observations (Brenner et al., 1984; Xu et al., 1987; Brenner, 1990) all indicate significant but transient binding of myosin heads to actin in a rapid equilibrium state commonly referred to as a "weak-binding" state. It is very likely that this is a state of nonstereospecific binding of myosin heads to actin; but it may not necessarily be involved in the active cross-bridge cycle.

On the basis of these two states, and the ideas of Huxley and Simmons (1971), a contraction mechanism has been postulated (Eisenberg and Hill, 1985) in which the cross-bridge cycle consists of myosin heads attaching to actin first in a low-force (weak-binding?) state and then

Address correspondence to Dr. Squire.

in a high-force (strong-binding) state. The latter could be similar to the rigor state; evidence for a small (<20%) population of rigorlike heads during contraction comes from probe studies (Cooke et al., 1982; Nagano and Yanagida, 1984; Fajer et al., 1991]. Previous x-ray diffraction results from frog muscle have been interpreted in terms of myosin heads undergoing a low-force to high-force structural transition (Huxley and Kress, 1985), but it was concluded: (*a*) that the low-force state was different from the state induced by low ionic strength solutions, (*b*) that two structurally different states could not be demonstrated directly, and (*c*) that the lack of a large intensity increase in the actin layer lines in x-ray diffraction patterns from contracting muscle could not be explained.

Here, we present results from active fish muscle. Preliminary and incomplete analysis of these results has been published elsewhere (Harford and Squire, 1990; Harford et al., 1991). The results presented here incorporate a great deal of new data, analyzed using more rigorous methods than earlier, together with analysis of the myosin layer-line pattern. The effects of possible sarcomere shortening have also been considered. These data are interpreted largely along the lines established in the seminal work of H. E. Huxley and his collaborators (Huxley and Brown, 1967; Huxley, 1968; Haselgrove and Huxley, 1973; Huxley, 1975; Huxley and Kress, 1985; Kress et al., 1986; Xu et al., 1987; Huxley et al., 1980; 1982), but also using other well-tried methods in crystallography, together with our own previous analysis of fish muscle diffraction data (Harford and Squire, 1986; 1990).

MATERIALS AND METHODS

Muscle preparation

Whole fin muscles from turbot, mounted in 10 ml perspex cells with mylar windows, were bathed in an oxygenated Ringer solution, derived from plaice blood serum (Cobb et al., 1973), at 5–8°C. Stimulation of muscles was by platinum wires running either side of and parallel to the length of the specimen. A sinusoidal 50 Hz ac field was applied to produce tetani of duration between 300 and 700 ms. Data were accumulated typically through 10 or 20 repeated cycles of contraction.

Camera design

Two-dimensional diffraction patterns were recorded on line 2.1 at the Daresbury Synchrotron Radiation Source (SRS, Warrington, UK). Beam line 2.1 comprises a mirror-monochromator camera design (Bordas et al., 1980), here with a specimen to detector distance of 3.2 m. Using the two-dimensional detector (512 × 512 image pixels; wire to wire resolution of 1 mm; maximum count rate 5×10^5 cps), the recorded intensities were channeled electronically (Hendrix et al., 1982) into separate time bins. Excellent intensity statistics were obtained throughout the two-dimensional diffraction pattern in 300 ms periods during the tetanus plateau and post- and pre-active (i.e., resting) plateau regions. One-dimensional (equatorial) patterns were recorded using a multiwire linear position sensitive detector (Hendrix et al., 1982) on line X33 at DESY, Hamburg. Data collected during one contraction were channeled into up to 256 separate time bins of 5 ms duration. A typical contraction cycle lasting 1.3 s included a 300 to 700 ms stimulation period. Usually data from 20 such cycles were added to give good statistics.

Data reduction

After correction for the detector response and subtraction of instrumental background, the specimen background was fitted with a Lagrangian polynomial function and subtracted. The remaining peaks were fitted with overlapping Gaussian profiles for the 100, 110, 200, 210, and 300 reflections and also the Z-line peak using a least-squares refinement to give the best fit (Harford and Squire, 1990). Because muscles used with the one-dimensional detector could be sorted into two groups with slightly different tension rise-times on activation, the results shown here are all from four muscles in one of these groups (eight half equatorial profiles). Because of the high intensity of the equatorial reflections, it was thought to be appropriate to pool data from a small number of experiments with exactly the same tension time course, rather than to dilute the data unnecessarily. The integrated counts recorded for the 100 reflection were ~220,000 giving an expected statistical accuracy of 0.2%. Comparable numbers for the relatively weak 300 reflection were 8,000 counts and an accuracy of ~1%. The time-courses of the 100 and 110 equatorial reflections were obtained only if both halves of the equator showed similar changes; data shown are %age changes of the raw intensity averaged over the four muscles, with 0 and 100% representing intensities in the resting and fully-active (well into the tetanus plateau) states. Results for the much weaker layer-line patterns recorded on the 2-dimensional detector were pooled from experiments with 15 muscles (60 quadrants). These 15 corresponded to those patterns with similar intensities in all four quadrants. Asymmetric diffraction patterns were discarded. Very high quality and reproducible intensities were obtained for both equatorial and layer-line regions.

Electron density maps

Electron density maps were computed by Fourier synthesis using the 100, 110, 200, 210, and 300 equatorial reflections with previously determined phases (Harford and Squire, 1990) using the expression $\rho(x, y) = \Sigma(\pm)F(h, k)\{\cos[2\pi(hx + ky)]\}T(h, k)$, assuming that $F(00)$ is constant. All maps were calculated using absolute intensity values which were all scaled to the intensity of the 100 reflection from resting muscle. $T(h, k)$ was a standard temperature factor $[\exp(-B \sin^2 \theta/\lambda^2)]$ with $B = 20{,}000$ Å^2. Trial maps were also computed with assumptions other than (*a*) that $F(00)$ is constant. If the density $[\rho(x, y)]$ in any map has a maximum ρmax and a minimum ρmin, then alternative assumptions could be: (*b*) that (ρmax − ρmin) for all the maps (i.e., for all times t) does not change, or (*c*) that the total density in the maps $[M = \Sigma\rho(x, y)]$ is constant for all t. Assumption (*b*) requires both that the highest density, actually always at the middle of the myosin filament backbone ($x = 0$, $y = 0$), never changes and that the minimum density seen is constant; probably always representing the density of the solvent. There seems to be no good reason, a priori, why either of these density levels should be constant. Both this assumption (*b*), and also assumption (*c*), may not be acceptable because of the possibility of changing "hidden" mass, as discussed by Yu et al. (1985). The assumption (*a*) that we prefer, with $F(00)$ constant, allows variations in "hidden" mass and in the myosin filament backbone. In this case the ρmax − ρmin values were each determined from the absolute intensity values for time t. The final densities were calculated, without being scaled to results from any other map, by first shifting the lowest ρmin observed in any of the maps for any time t to zero by an amount $\Delta\rho$ and then shifting all the ρ values in all the maps by exactly this same amount $\Delta\rho$. As it happens, this method is not only theoretically more sound but it gave much more reproducible, less noisy, results than with the other assumptions. Furthermore, although constancy of total mass had not been assumed, both a virtually constant M and a virtually constant myosin backbone peak density resulted.

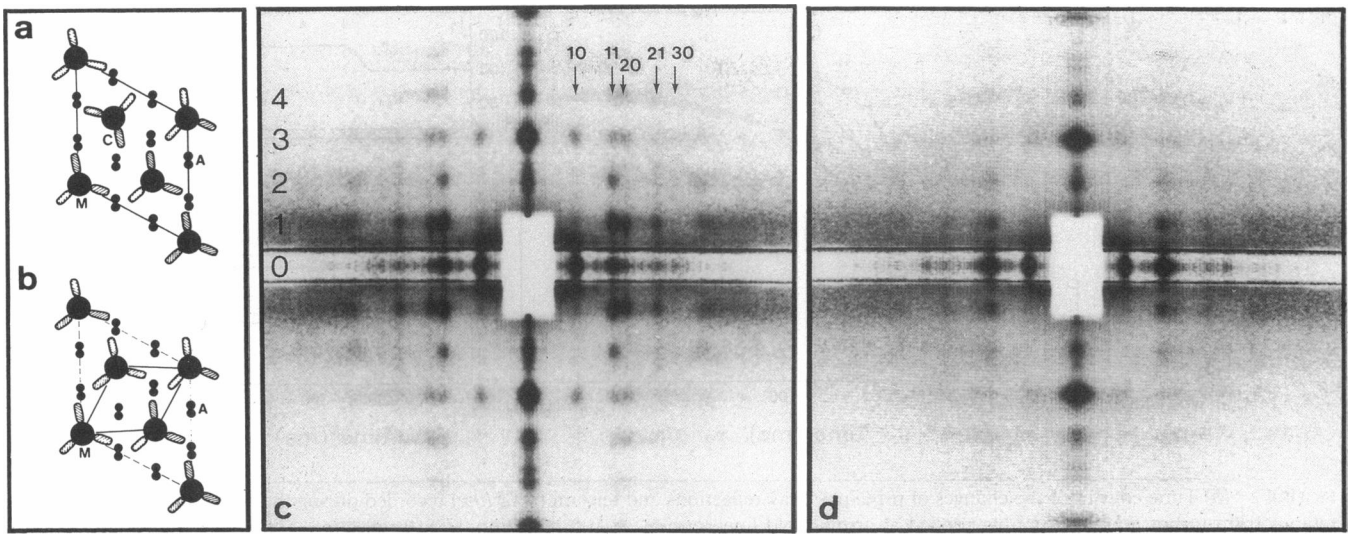

FIGURE 1 (*a, b*) Schematic representations of end-on views of the lattice of thick myosin-containing filaments (M) and thin actin-containing filaments (A) in vertebrate skeletal muscles. A single level of the three-stranded helical array of myosin cross-bridges (C) is represented. Thick filaments with one of two different orientations form a statistical superlattice in most vertebrate muscles (*a*), whereas in teleost fish muscles (*b*) such filaments have a single orientation and form a simple lattice (*unbroken line*). The regular three-dimensional cross-bridge lattice in teleosts gives simple layer-line sampling in the x-ray diffraction patterns (*c, d*) from live turbot (*Scopthalmus maximus*) fin muscle (*fiber axis vertical*) recorded using a fast two-dimensional multiwire detector on line 2.1 at the Daresbury synchrotron; (*c*) resting muscle, (*d*) fully-active muscle (6 s accumulated exposure in each, with the synchrotron source at 2.00 GeV and ~150 mA). Intensities in *c* and *d* have been scaled by the distance from the center of the pattern to enhance visibility of the outer reflections. Layer lines (*horizontal*) are indicated as 0–4; the numbers represent orders of 42.9 nm. The third order corresponds to 14.3 nm. An attenuation strip along the equator (*central horizontal band*) reduced the intensity of the very strong equatorial reflections. Row lines (*vertical*) are labeled as 10, 11, 20, 21, and 30. Note the intensity drop of the layer lines in *d* compared with *c*, the increase and broadening of the meridional 14.3 nm reflection and the intensity changes of the 100, 110, and higher order equatorial reflections.

Note finally that the time courses shown in Fig. 2 are not the same as those previously published, for example, as Fig. 6 in Harford et al. (1991) or as Fig. 10.14 in Harford and Squire (1990). Intensities shown here in Fig. 2 *a* were more rigorously fitted than before, giving much smoother time courses, and the mass time course in Fig. 2 *a* was computed (as discussed above) assuming $F(00)$ is constant, as opposed to the previous assumption (which we now consider less valid) that ρmin and ρmax were constant.

RESULTS

X-ray diffraction observations on fish muscle

Fig. 1, *c* and *d*, show typical low-angle diffraction patterns from resting and fully active turbot fin muscle recorded using the two-dimensional multiwire detector on line 2.1 at the Daresbury SRS. These patterns show the regular sampling of the myosin layer lines to at least 7 nm resolution (orders of 42.9 nm labeled $l = 0, 1, 2, 3$, et cetera). The sampling is along "vertical" row lines (hk = 10; 11; et cetera) arising from the highly ordered hexagonal lattice of myosin filaments in the fish muscle A-band (Luther and Squire, 1980; Harford and Squire 1986, 1990). Most vertebrates have a superlattice A-band unit cell (Fig. 1 *a*) with statistical disorder (Luther and Squire, 1980), whereas teleost muscles (Fig. 1 *b*) have a regular simple lattice of the three-stranded helical myosin filaments (Luther and Squire, 1980; Harford and Squire, 1986, 1990).

The equator of the fish muscle diffraction pattern (l = 0 in Fig. 1 (*c* and *d*); reflections of the type $h, k, 0$) provides information about the muscle A-band when viewed in projection down the fiber axis. The 100 and 110 reflections have been shown previously to be sensitive to myosin cross-bridge movement (Huxley and Brown, 1967; Haselgrove and Huxley, 1973). Thus, when myosin heads move from the quasi-helical arrangement on myosin filaments in resting muscle (Huxley and Brown, 1967; Squire, 1981; Harford and Squire, 1986) to attach to actin in active or rigor muscle, the 100 intensity reduces and the 110 gets stronger (Fig. 1 *c, d;* Huxley, 1968). For this reason, the 110 intensity increase has been taken as an indicator of cross-bridge attachment to actin. However, because the configuration of the heads on actin also affects this intensity (Lymn, 1978), it is important to remember that the 110 intensity does not give a direct measure of the number of attached heads.

Fig. 2 *a* shows the normalized intensity time-courses of the 100 and 110 reflections from contracting turbot muscle as determined from 5-ms time frames recorded using the very fast linear detector (Hendrix et al., 1982) on line X33 at DESY, Hamburg. Care has been taken to separate, using curve-fitting procedures (Harford and Squire, 1990), the 110 reflection from the 200 reflection and the Z-line peak (d = 27 nm) with which it overlaps

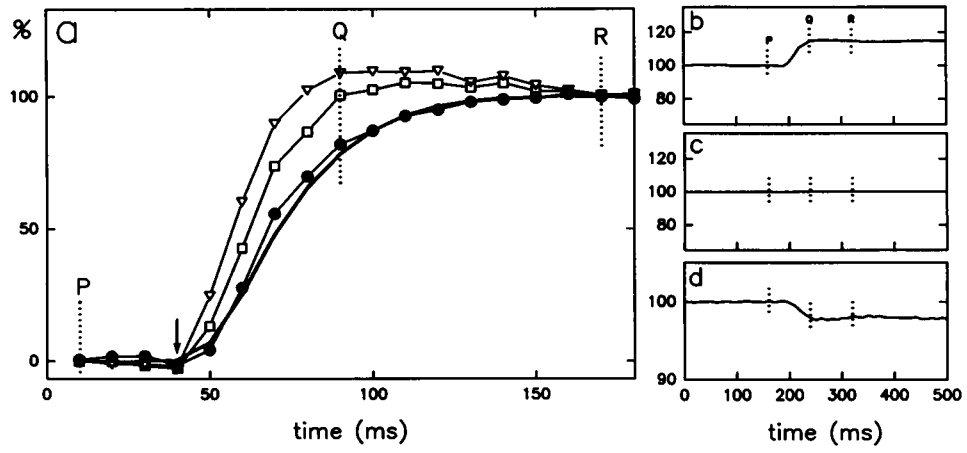

FIGURE 2 (*a*) Time courses of the changes of principal x-ray reflections and tension (*bold line*) recorded during the rising phase of an isometric tetanus from turbot muscle (stimulus applied at arrow, bold line; tension, ● 100 reflection, ▽ 110 reflection). The mass time course (□) was determined from Fourier synthesis maps (see Fig. 3) using the first five equatorial reflections (100, 110, 200, 210, 300) at 10 ms time intervals. Shown is the mass within 9 nm of the actin filament axis (see Fig. 3 *d*). Phases used were 0, 0, π, 0, 0, respectively. Note that all time courses have been normalized to 0% during the initial resting phase using the mean over 300 ms near to point *P* and to 100% using mean values during 300 ms of the tension plateau (near point *R*). *P*, *Q*, and *R* represent specific times during the tetanus referred to in the text. (*b*, *c*, and *d*) Time courses of percentage changes over a wider time range than *a* of: *b* the total mass within 9 nm of the actin filament axis (cf. *a*; maximum change ~15%), (*c*) the total mass within the whole unit cell from maps such as those in Fig. 3 (no detectable change), and (*d*) the change (maximum 2%) in spacing of the 100 equatorial reflection (i.e., the reciprocal of the 100 spacing in the hexagonal A-band lattice (cf. Fig. 1, *a* and *b*). Points *P*, *Q*, and *R* in *c* to *d* correspond to *P*, *Q*, and *R* in (*a*).

(Yu et al., 1977; Harford and Squire, 1986). This provides highly reliable intensity data that are consistent between the chosen experiments. The time courses of the changes of the 100 and 110 reflections are quite different; there is no theoretical reason why they should be the same. The 100 intensity decrease (plotted upwards in Fig. 2 *a*) has a rather similar time course to the increase of the recorded tension (there may be a very small lead; ~5 ms). Half-maximal change in the 100 intensity occurs about $t_{1/2} = 35 \pm 8$ ms after activation. On the other hand the 110 intensity increases very rapidly on activation such that it reaches 50% of its final steady-state value at the tension plateau (used for scaling) about $t_{1/2} = 21 \pm 4$ ms after activation and 20 ms before the recorded tension reaches 50% of its plateau value ($t_{1/2} = 41 \pm 3$ ms post stimulus).

It is conceivable that the recorded tension is artificially delayed due to the take up of slack along the muscle length, and also that a changing sarcomere length could itself modify the equatorial intensity distribution due to the changing filament overlap. However, our evidence to date is that this effect is small; there is only a very small increase in A-band lattice spacing (<2%) during typical tetanic contractions (Fig. 2 *d*). This could be due either to radial effects of the cross-bridge interaction or to sarcomere length reduction. If it was entirely a sarcomere effect then a 4% reduction in sarcomere length would be involved, which would be associated with an increase in total mass in the A-band lattice. As discussed later, we see no detectable increase in total A-band mass (Fig. 2 *c*) during the lattice spacing change. Furthermore the change in lattice spacing is over (point *Q* in Fig. 2) while the 100 and 110 equatorial intensities are still changing. We believe that the differences between the time courses of the 100 and 110 reflections are real, because, at the time of 50% change in the tension, the measured intensity changes for the 100 and 110 reflections are 56 ± 11% and 89 ± 6% respectively; they are very significantly different. For these various reasons we have ignored the possibility of a substantial effect of sarcomere shortening in the arguments which follow. However, these arguments would not be markedly affected if the tension record was artifactually delayed by, say, 5 ms due to sarcomere length shortening. Other published evidence on the effects of sarcomere clamping has shown that the main effect of clamping is to move all of the observed time courses to the left, without markedly changing their sequence or relative separation (Cecchi et al., 1991).

Changing mass distributions in the A-band unit cell

Using the 110 intensity as a general indicator of myosin head attachment to actin (but not as a direct measure of the number attached [Lymn, 1978]), the rapid change of the 110 intensity before the recorded tension has changed a great deal seems to imply that at an early stage in the activation process there are many myosin heads attached to actin in a state which produces little force. Such a build-up of cross-bridge mass near actin when the recorded tension is still low can be demonstrated more directly by computing Fourier synthesis electron density map images of the A-band unit cell. Such maps have been computed for 10-ms intervals during the rising

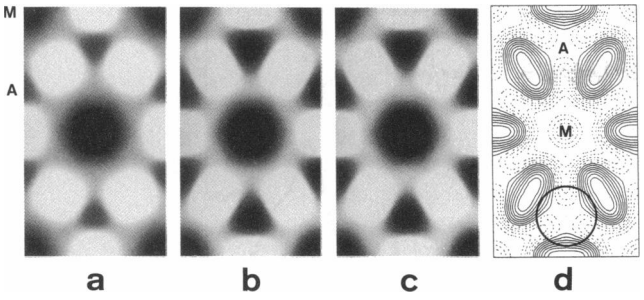

FIGURE 3 (*a*, *b*, and *c*) Fourier synthesis electron density maps computed using equatorial data from isometrically contracting turbot muscle computed for 10 ms time intervals and corresponding to times *P*, *Q*, and *R* respectively in Fig. 2; dark is protein density. All maps were computed using absolute intensity values. They were then shifted by the same amount to make the lowest density in any of the maps equal to zero and were subsequently scaled by the same factor to make the myosin origin density at time *P* (i.e., in *a*) equal to 100. (*d*) Density difference map ×50: Map *c* minus Map *b*; solid contours show density increases, broken contours show density loss. Density changes at the axes of the myosin (M) and actin (A) filaments are small. Main changes are density loss in a ring around M and density gain between adjacent actin filaments. The circle in (*d*) shows the radius within which actin mass was counted for Fig. 2, *a* and *b*.

phase of contraction using the intensity data on the first five equatorial reflections (100, 110, 200, 210, 300). Three examples of such maps, corresponding to points *P*, *Q*, and *R* in Fig. 2, are shown as Fig. 3 (*a–c*) respectively. To produce maps as free as possible from artifact (termination errors) at 13-nm resolution (Yu, 1989), the observed equatorial amplitudes have been modified by the well-tried crystallographic procedure of applying an artificial (Gaussian) temperature factor (B = 20,000 Å^2) to avoid series termination artifacts in the computed density maps (Harford and Squire, 1990; Franks et al., 1982). Detailed interpretation of maps computed without this precaution is unsafe.

The phases needed to compute these maps have not been determined directly, but we have argued in detail elsewhere (Squire, 1981) that the A-band structure possesses three-fold rotational symmetry around the fiber axis and is centrosymmetric at 13-nm resolution. This means that possible phase values are restricted to 0 or π. Of the possible phase combinations, the most likely set for fish muscle (Harford and Squire, 1990) is 0, 0, π, 0, 0. However, just plausible is an alternative set 0, 0, π, π, 0. We have argued elsewhere (Harford and Squire, 1990) the reasons for these choices of phase; it is extremely unlikely that in the case of fish muscle, the phases could be any different from these two possibilities. As it happens, when the computed density maps are used to show the total mass within about 9 nm radius of the actin filament axis at any instant during the tetanus (Fig. 2, *a* and *b*), then the mass time courses generated using the two preferred phase sets are almost identical; the conclusions below are the same whether the 210 phase is 0 or π. In addition, no sharp intensity discontinuities during the active period, consistent with a change of phase of any of these reflections, have ever been observed.

The time after stimulus for the mass accumulation at actin to reach 50% of its steady-state value (Fig. 2 *a*) is $\sim t_{1/2}$ = 25 ms. There is a lead of ~10 ms compared with the time course of the equatorial 100 reflection and a 10–15-ms lead in mass accumulation at actin relative to the recorded tension. The mass at actin reaches a steady level at point *Q* in Fig. 2 (*a–d*), even when the recorded tension is still rising. This must mean that there are many heads attached to actin at points just before and up to *Q* in Fig. 2 (25–50 ms after activation) with a relatively low force produced, but associated with a relatively strong 110 intensity. This observation is entirely consistent with previous mechanical measurements of other muscles (Huxley and Simmons, 1971; Brenner et al., 1982; Ford et al., 1986). After this (between points *Q* and *R*), the 110 intensity remains high, the mass accumulated within 9 nm of the actin axis remains constant, but the 100 intensity gradually reduces for a further 20 to 30 ms. This is most easily explained if there is roughly the same number of heads attached to actin, but if some of these attached heads have changed their configuration on actin (Lymn, 1978). At the same time, the force produced increases substantially. We envisage a structural scheme:

$$A + M \rightleftharpoons \begin{matrix} AM^1 \\ \rightleftharpoons \\ AM^2 \end{matrix}$$

(where AM^1 and AM^2 are the average structures of low-force and high-force attached cross-bridge configurations respectively and the nucleotide state is not specified). Our results can be explained if, after *Q*, the sum of the populations in the two attached configurations remains constant, but the population in AM^2 increases while AM^1 reduces. It seems reasonable to equate configurations AM^1 and AM^2 loosely with the low-force and high-force cross-bridge states of previous studies (Huxley and Simmons, 1971; Huxley and Kress, 1985; Ford et al., 1986; Yu and Brenner, 1989; Brenner, 1990; Cecchi et al., 1991). However, it is by no means clear that these structural states AM^1 and AM^2 can be correlated exactly with specific biochemical states, because, for example, a head in the biochemical state AM (i.e., no nucleotide) could be in state AM^2 (e.g., rigorlike) or could be distorted back to structural state AM^1 because of elasticity in the head/actin assembly.

Initial (low-force) attachment state

A clue to the cross-bridge configuration predominating when the force is low comes from the work of Matsuda and Podolsky (1984) who showed that muscles in the weak-binding state produced by low ionic strength solutions still appeared to show a myosin layer line pattern

(based on a 42.9-nm repeat) and little enhancement of the actin layer line pattern (based on a 37-nm repeat). We have shown elsewhere by modeling studies (Squire and Harford, 1988) that the Fourier transform of an array of heads attached to actin nonstereospecifically while remaining myosin-centered (e.g., as in the weak-binding state; see later discussion and Fig. 5 *b*) will still give rise to myosinlike layer lines (at about 42.9, 21.5, and 14.3 nm). Only when the heads become stereospecifically bound to actin (e.g., as in a strong-binding state; Fig. 5 *c*), will the actin layer lines become intensified (Squire and Harford, 1988). In the present study, the myosin layer lines at 42.9, 21.5 nm and so on became substantially weaker when the muscle was activated (Fig. 1, *c* and *d*), as previously reported for contracting frog muscle (Huxley and Brown, 1967; Huxley et al., 1980) an observation consistent with the centers of mass of the myosin heads moving away from the resting helical array (Huxley and Brown, 1967). The time course of the intensity change (drop) of the 111/201 reflections on the myosin first layer line is similar to that of the mass time course (time for 50% change 25 ± 6 ms). After the very rapid Ca^{2+}-activation events in muscle (Ashley et al., 1991), this change in the 111/201 reflection signals a relatively early structural event. However, there is not just a general drop in first layer-line intensity. There is a clear first layer-line remnant with substantial changes in relative intensity along it; the 201-peak decreases less than the 111 peak (Fig. 4). The ratio I_{111}/I_{201} changes from 2.9 ± 0.46 in resting patterns to 1.35 ± 0.68 in patterns from fully-active muscle.

This change does not appear to be due to a change in the relative intensities of the myosin 42.9-nm layer line and the inner end of the actin 37-nm layer line, which might conceivably overlap in this region, because no discernible change in the mean axial spacing of the layer line at the 111/201 row-line position has been observed. The profile fits to the 111 and 201 peaks in Fig. 4 (*a* and *b*) also show only a small change in the sampling of the layer line, as indicated by only a small change in row-line width. Considering other factors that could affect the layer-line intensity, no change in the relative intensities of the 111 and 201 reflections would be expected if either a fraction of the heads on each myosin filament became disordered whereas the remaining heads remained in their original positions on the myosin helix, or if only part of the muscle was activated, and part remained relaxed, or if different thick filaments lost their helical order in a cooperative manner, but at different times. If the heads remained with the same mean configurations (tilt and slew) on the filament surface, but the radial directions out to the head origins became generally azimuthally disordered about their mean helical positions, then the outer parts of the myosin layer lines would be expected to drop in intensity more than the inner parts, not less as observed. With these possibilities excluded, it seems most plausible that the preferential decrease of the low radius 111 reflection relative to the higher radius 201 reflection must be showing that the outer ends (proximal to actin) of the myosin heads move more off the resting helix than the inner ends (proximal to myosin). Such a modified layer-line pattern based on the 42.9-nm repeat is consistent with myosin heads making nonstereospecific interactions with actin (Fig. 5 *b*); the head configuration could be similar in geometry to the one postulated to occur in the low-ionic strength weak-binding state (Yu and Brenner, 1989; Brenner, 1990; Harford and Squire, 1990). Here, the myosin rod ends of the heads

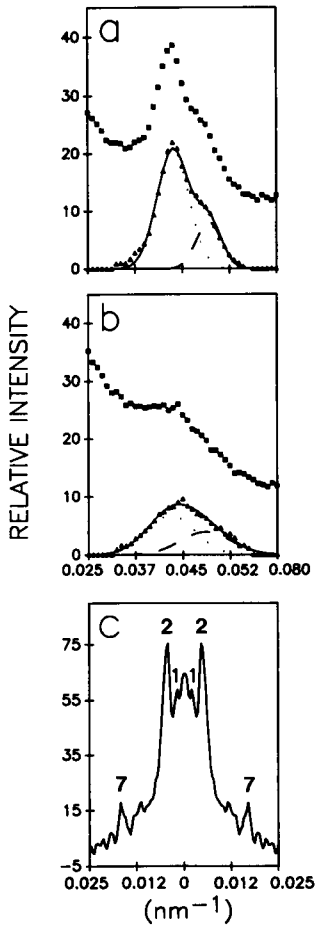

FIGURE 4 Intensity profiles along the first myosin layer line (l = 1) at 42.9 nm in the x-ray diffraction pattern from (*a*) live (resting) turbot muscle and (*b*) isometrically contracting muscle recorded using the area detector (see Fig. 1, *c* and *d*). These correspond to averaged profiles from 15 muscles (60 half layer-line profiles) for part of the top right hand quadrant in Fig. 1 (*c*, *d*); the meridian is to the left of each trace. (Key: [■] observed data; [▲] observed data with the Lagrangian polynomial background subtracted; [—] sum of modeled Gaussian peaks; [· · · · ·] 110 modeled peak; [– – – –] 200 modeled peak). (*c*) Intensity difference profile recorded using the one-dimensional detector parallel to the meridian and crossing the actin layer lines (first, second, and seventh orders of ~37 nm are labeled) at a radial position centered at ~1/4.5 nm^{-1}. The difference is obtained by subtracting the resting diffraction pattern from the active (tetanus plateau) intensity data. Large intensity increases can be seen on the first and second layer lines (37 and 18.5 nm, respectively) as can small increases on some of the higher angle actin layer lines.

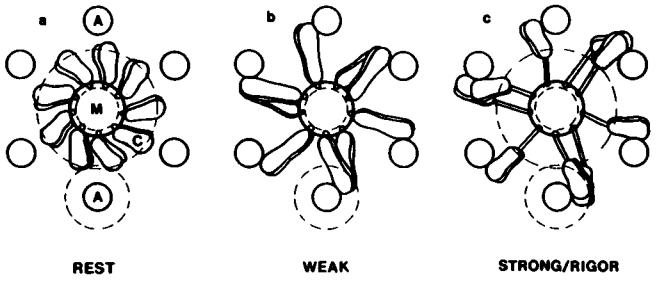

FIGURE 5 Models showing the postulated myosin head (C) configurations relative to the myosin filament backbone (M) and actin filament (A) for; (*a*) resting muscle, (*b*) the low-force state (AM^1), (*c*) the high-force state (AM^2), which may be rigor-like (see also Fig. 8 in Yu and Brenner, 1989). The dotted circles centered on the actin filament positions show the 9-nm circle relating to the actin mass time course in Fig. 2. The heads appear shorter in (*a*) and (*c*) than in (*b*) because they are assumed to be tilted axially and thus, to be foreshortened. The density difference map in Fig. 3 *d* corresponds qualitatively, we argue, with a population of heads moving from structure (*b*) to structure (*c*).

are still myosin-centered (i.e., well ordered in their resting positions on the thick filament surface), but their outer ends proximal to actin have become azimuthally disordered due to actin attachment in a nonstereospecific manner (Fig. 5 *b*). Note that these low-force bridges probably have a similar structure to the previously observed weak-binding bridges (Yu and Brenner, 1989), but the present work can say nothing about the kinetic properties of this state.

Later (high-force/strong) attachment state

The existence of myosin heads strongly and stereospecifically attached to actin must have its effect on the intensities of the actin layer lines. However, work on the activation of muscle thin filaments at nonoverlap sarcomere lengths (Yagi and Matsubara, 1989) has shown that, even in the absence of myosin head interaction, activation-related changes do occur on the actin layer lines. In particular, there is a marked intensity increase of the second actin layer line at 18 nm, associated with a tropomyosin shift involved in regulation (Haselgrove, 1973; Huxley, 1973; Parry and Squire, 1973), and there are changes on the 5.9 and 5.1-nm layer lines. Such changes also occur in fish muscle diffraction patterns, as shown in the difference trace in Fig. 4 *c* from active turbot muscle at full overlap; a large change on the second actin layer line and smaller changes on the first layer line and some of the higher order layer lines can be seen. Modeling studies reported elsewhere (Yagi and Matsubara, 1989; Yagi, Matsubara and Squire, manuscript in preparation) have shown that the intensity changes on the 5.9-nm and other higher order layer lines from nonoverlap muscles can be explained by a relative movement of the domains of the actin monomer. In full-overlap muscles, where myosin head interaction can also occur, the effect of labeling by myosin heads will be superimposed on these structural changes within the thin filament system (although myosin head labeling may also modify the inherent changes in the actin filament). Thus small further increases on the 5.9-nm layer line and other layer lines may occur due to myosin head labeling. In x-ray diffraction patterns from rigor muscle, the most obvious intensity increase is on the first actin layer line at 37 nm (Huxley and Brown, 1967) and this is particularly marked because of the pseudo-periodic (ladderlike) labeling of the actin helix in actin target areas spaced at 37 nm axial intervals (Squire and Harford, 1988). However, in x-ray patterns from fully-active muscle, in which a substantial population of the myosin heads must label actin, at most only small changes of the 37-nm layer line have been reported (Huxley et al., 1982; Matsubara et al., 1984; Wakabayashi et al., 1988, 1991). The changes reported by Wakabayashi et al. (1991) depended both on the degree of overlap of the muscle and the particular radial position along the layer line. It now seems likely that the small observed first layer line change in patterns from active muscle is partly due to the fact that the intensification of the second actin layer line due to tropomyosin movement is associated with a marked intensity decrease on at least part of the first actin layer line at 37 nm (Haselgrove, 1973; Huxley, 1973; Parry and Squire, 1973; Yagi and Matsubara, 1989; Yagi, 1991). Thus, without any myosin head labeling, one would expect a significant part of the 37-nm layer line to get much weaker in patterns from active muscle. However, another contributory factor to this is that the marked intensification of the first actin layer line close to the meridian in patterns from rigor muscle is not just due to the fact that there is extra mass, the myosin heads, at a relatively high radius around actin, but, as discussed by Squire and Harford (1988), is due to the specific (ladderlike) pattern of labeling of the myosin heads on 37 nm-spaced actin target areas. Labeling in active muscle is likely to be much less ladderlike (Squire, Alkhayat and Harford, manuscript in preparation) and will not produce the same kind of diffraction at the inner end of the first actin layer line as the rigor labeling. In our studies of changes of the second actin layer line (Fig. 4 *c*), we noted a slight intensity increase in the outer part of the first layer line, where little change was reported by Yagi and Matsubara (1989) in patterns from nonoverlap frog muscle. The observation of even a small increase of this layer line (e.g., Fig. 4 *c*) at this radial position ($1/4.5\ nm^{-1}$), an observation also reported by Wakabayashi et al. (1991) for frog muscle, probably shows either that a mass increase due to stereospecific labeling of actin by myosin heads has contributed here, or that the head labeling has itself altered the actin filament structure; a conclusion very different from that reached by Huxley and Kress (1985).

Fourier difference density and cross-bridge swinging

The equatorial Fourier synthesis difference map (Fig. 3 *d*) between times *Q* and *R* in Fig. 2, where the same mass

is actin attached within 9 nm radius, but the force produced is different, shows that the transition from initially attached (low force) heads (Q) to a greater population of high force heads (R) is associated with a characteristic change in the projected distribution of mass. There is virtually no density change on the axis of the myosin (M) and actin filaments (A), as might be expected. However, despite the constancy of the total mass within 9 nm of the actin axis, which we take to imply a roughly constant number of attached heads, there is further loss of mass from around the myosin filament and an increase at the positions between adjacent actin filaments. We interpret this as an indication of a shift in attachment configuration of a population of myosin heads from our suggested low-force conformation (AM^1; Fig. 5 *b*), where substantial mass remains near to the myosin filament, to the strong-binding, force-producing state (AM^2; Fig. 5 *c*), where the head mass is especially enhanced in the position between adjacent actin filaments. Further analysis of the modified myosin layer-line pattern and the active actin layer-line pattern from fish muscle will help to test, confirm and elaborate this interpretation.

CONCLUSION

We conclude that a low-force actin-attached cross-bridge state (or states) exists in which myosin heads are still myosin-centered, they contribute to a myosinlike layer-line pattern different in intensity distribution along the myosin layer lines from the resting pattern and they cause a larger change in the 110 equatorial reflection than in the 100 reflection. At a later time during the rising phase of the tetanus, a greater population of the attached heads goes over to a structurally different high-force state (or states), which contributes less to the myosin layer-line pattern because it is actin-centered. Because of stereospecific binding to actin, these heads contribute more to the actin layer-line pattern, but the intensity change that is seen is very much less than in patterns from rigor muscle because (*a*) a reduction in intensity of the first actin layer line at high radius due to activation (possibly associated with tropomyosin movement) has to be compensated for before an increase in this position along the layer line will be seen and (*b*) the ladderlike pattern of labeling of the actin target areas seen in rigor muscle, which contributes strongly to the meridional end of the first actin layer line (Squire and Harford, 1988), is much less well developed in active muscle. The small observed increase in Fig. 4 *c* is either a direct or an indirect indication of stereospecific actin attachment by myosin heads. The high-force/strong-binding heads are associated with only a slight further strengthening of the 110 equatorial reflection, but a much reduced 100 intensity compared with the low-force heads.

It is not clear yet whether our postulated low-force heads correspond to the nonstereospecifically attached heads observed by Berger et al. (1989), Barnett and Thomas (1989), Fajer et al. (1991) and Stein et al. (1991). In our case, these heads are taken to give rise to the modified myosin first layer line, but a large spread in the axial tilt of the heads would be expected to reduce radically the myosin layer-line intensity. Modeling of the x-ray data will test this point.

The redistribution of projected mass (Fig. 3) in the A-band unit cell between our chosen times Q and R in Fig. 2, as indicated by the difference map in Fig. 3 *d*, appears to require either a change in head shape, against which there is much contrary evidence (Curmi et al., 1988; Vibert, 1988), or an axial component of head movement. As detailed elsewhere (Squire, 1988), this swinging could be associated with a rotation of most or all of the head close to the actin/myosin interface, or to swinging of the whole head which is attached rigidly to an outer domain of actin (Squire, 1988; Kabsch et al., 1990) which itself rotates relative to the other domains. Such swinging is the most plausible explanation and would explain directly the origin of the sliding force between the actin and myosin filaments.

As discussed above, it is not at all clear, as yet, how these two states (or groups of states) relate to the identified biochemical intermediates in the actomyosin ATPase cycle (Eisenberg and Hill, 1985; see Brenner [1990] for review). The problem is both that heads in different biochemical states could have virtually the same structural state and that heads in a single biochemical state could be in various stages of distortion and therefore belong to either of the observed structural states. It is hoped that further structural analysis of fish muscle diffraction data will help to clarify this issue.

Note finally that the relatively wide time separation of the 100 and 110 changes, possibly wider than seen with other muscles (Huxley, 1975; Brenner, 1990; Cecchi et al., 1991; Bordas et al., 1991), may be a genuine species effect associated with the different regulatory properties of fish muscle (Harford, Alkhayat and Squire, manuscript in preparation); an effect which is helping in the separation of low-force and high-force states.

We are very much indebted to Dr. Yuichiro Maeda at the European Molecular Biology Laboratory (EMBL) Outstation, DESY, Hamburg and to Dr. Liz Towns-Andrews at the Daresbury Synchrotron Radiation Source for their willing and expert help and advice in setting up the beam-lines for these experiments. We also thank Professor Joan Bordas (Daresbury Laboratory) for his constant support and encouragement, and the staffs at the Medical Research Council/Science and Engineering Research Council Biological Support Laboratory at Daresbury and the EMBL Outstation at Hamburg for their excellent technical support. These experiments were initiated with the advice of Drs. H. E. Huxley and A. R. Faruqi to whom we are indebted. Finally, we record with appreciation discussions that we have had over a period of years with Drs. Leepo Yu and Bernhard Brenner about the interpretation of their mechanical and x-ray diffraction studies of muscles in the weak-binding state produced by low-ionic strength solutions.

This work was funded by Programme and Project grants from the British Medical Research Council and short term fellowships from EMBO.

Received for publication 5 November 1991 and in final form 26 March 1992.

REFERENCES

Ashley, C. C., I. P. Mulligan, and T. J. Lea. 1991. Ca^{2+} and activation mechanisms in skeletal muscle. *Q. Rev. Biophys.* 24:1–73.

Barnett, V. A., and D. D. Thomas. 1989. Microsecond rotational motion of spin-labeled myosin heads during isometric muscle contraction: saturation transfer electron paramagnetic resonance. *Biophys. J.* 56:517–523.

Berger, C. L., E. C. Svensson, and D. D. Thomas. 1989. Photolysis of a photolabile precursor of ATP (caged ATP) induces microsecond rotational motions of myosin heads bound to actin. *Proc. Natl. Acad. Sci. USA.* 86:8753–8757.

Bordas, J., M. H. J. Koch, P. N. Clout, E. Dorrington, C. Boulin, and A. Gabriel. 1980. A synchrotron radiation camera and data acquisition system for time-resolved x-ray scattering studies. *J. Phys. E. Sci. Instrum.* 13:938–944.

Bordas, J., G. P. Diakun, J. E. Harries, R. A. Lewis, G. R. Mant, M. L. Martinez-Fernandez, and E. Towns-Andrews. 1991. Two-dimensional time resolved x-ray diffraction of muscle: recent results. *Adv. Biophys.* 27:15–33.

Brenner, B. 1990. Muscle mechanics and biochemical kinetics. *In* Molecular Mechanisms in Muscular Contraction. J. M. Squire, editor. Macmillan Publishing, NY. 77–149.

Brenner, B., M. Schoenberg, J. M. Chalovich, L. Greene, and E. Eisenberg. 1982. Evidence for cross-bridge attachment in relaxed muscle at low ionic strength. *Proc. Natl. Acad. Sci. USA.* 79:7288–7291.

Brenner, B., L. C. Yu, and R. J. Podolsky. 1984. X-ray diffraction evidence for cross-bridge formation in relaxed muscle fibers at various ionic strengths. *Biophys. J.* 46:299–306.

Cecchi, G., P. J. Griffiths, M. A. Bagni, C. C. Ashley, and Y. Maeda. 1991. Time-resolved changes in equatorial x-ray diffraction and stiffness during rise of tetanic tension in intact length-clamped single muscle fibers. *Biophys. J.* 59:1273–1283.

Cobb, J. L. S., N. C. Fox, and R. M. Santer. 1973. A specific Ringer solution for the plaice. *J. Fish Biol.* 5:587–591.

Cooke, R., M. S. Crowder, and D. D. Thomas. 1982. Orientation of spin labels attached to cross-bridges in contracting muscle fibers. *Nature (Lond.).* 300:776–778.

Curmi, P. M. G., D. B. Stone, D. K. Schneider, J. A. Spudich, and R. A. Mendelson. 1988. Comparison of the structure of myosin subfragment 1 bound to actin and free in solution; a neutron scattering study using actin made 'invisible' by deuteration. *J. Mol. Biol.* 203:781–798.

Eisenberg, E., and T. L. Hill. 1978. A crossbridge model of muscle contraction. *Prog. Biophys. Mol. Biol.* 33:55–82.

Eisenberg, E., and T. L. Hill. 1985. Muscular contraction and free energy transduction in biological systems. *Science (Wash. DC).* 227:999–1006.

Fajer, P. G., E. A. Fajer, M. Schoenberg, and D. D. Thomas. 1991. Orientational disorder and motion of weakly attached cross-bridges. *Biophys. J.* 60:642–649.

Ford, L. E., H. E. Huxley, and R. M. Simmons. 1986. Tension transients during steady shortening of frog muscle fibers. *J. Physiol. (Lond.).* 372:595–609.

Franks, N. P., V. Melchior, D. A. Kirschner, and D. L. D. Caspar. 1982. Structure of myelin lipid bilayers. Changes during maturation. *J. Mol. Biol.* 155:133–153.

Harford, J. J., and J. M. Squire. 1986. "Crystalline" myosin cross-bridge array in relaxed bony fish muscle: Low-angle x-ray diffraction from plaice fin muscle and its interpretation. *Biophys. J.* 50:145–155.

Harford, J. J., and J. M. Squire. 1990. Static and time-resolved x-ray diffraction studies of contracting fish muscle. *In* Molecular Mechanisms in Muscular Contraction. J. M. Squire, editor. Macmillan Press, NY. 287–320.

Harford, J. J., M. W. Chew, J. M. Squire, and E. Towns-Andrews. 1991. Cross bridge states in isometrically contracting fish muscle: evidence for swinging of myosin heads on actin. *Adv. Biophys.* 27:45–61.

Haselgrove, J. C. 1973. X-ray evidence for a conformation change in the actin containing filaments of vertebrate striated muscle. *Cold Spring Harbor Symp. Quant. Biol.* 37:341–352.

Haselgrove, J. C., and H. E. Huxley. 1973. X-ray evidence for radial cross-bridge movement and for the sliding filament model in actively contracting skeletal muscle. *J. Mol. Biol.* 77:549–568.

Hendrix, J., H. Fuerst, B. Hartfiel, and D. Dainton. 1982. A wire per wire detector system for high counting rate x-ray experiments. *Nucl. Instrum. Methods.* 201:139–144.

Holmes, K. C., R. T. Tregear, and J. Barrington Leigh. 1980. Interpretation of the low angle x-ray diffraction from insect flight muscle in rigor. *Proc. R. Soc. Lond. B Biol. Sci.* 207:13–33.

Huxley, A. F. 1973. Muscle structure and theories of contraction. *Proc. Roy Soc. Lond. B Biol. Sci.* 183:83–86.

Huxley, A. F., and R. M. Simmons. 1971. Proposed mechanism of force generation in striated muscle. *Nature (Lond.).* 233:533–538.

Huxley, H. E. 1968. Structural differences between resting and rigor muscle. Evidence from intensity changes in the low-angle equatorial x-ray diagram. *J. Mol. Biol.* 37:507–520.

Huxley, H. E. 1969. The mechanism of muscular contraction. *Science (Wash. DC).* 164:1356–1366.

Huxley, H. E. 1973. Structural changes in the actin and myosin containing filaments during contraction. *Cold Spring Harbor Symp. Quant. Biol.* 37:361–376.

Huxley, H. E. 1975. The structural basis of contraction and regulation in skeletal muscle. *Acta Anat. Nippon.* 50:310–325.

Huxley, H. E., and W. Brown. 1967. The low-angle x-ray diagram of vertebrate striated muscle and its behaviour during contraction and rigor. *J. Mol. Biol.* 30:383–434.

Huxley, H. E., and M. Kress. 1985. Crossbridge behaviour during muscle contraction. *J. Muscle Res. Cell Motil.* 6:153–161.

Huxley, H. E., A. R. Faruqi, J. Bordas, M. H. J. Koch, and J. R. Milch. 1980. The use of synchrotron radiation in time-resolved x-ray diffraction studies of myosin layer-line reflections during muscle contraction. *Nature (Lond.).* 284:140–143.

Huxley, H. E., A. R. Faruqi, M. Kress, J. Bordas, and M. H. J. Koch. 1982. Time-resolved x-ray diffraction studies of the myosin layer-line reflections during muscle contraction. *J. Mol. Biol.* 158:637–684.

Kabsch, K., H. G. Mannherz, D. Suck, E. F. Pai, and K. C. Holmes. 1990. Atomic structure of the actin: DNase I complex. *Nature (Lond.).* 347:37–44.

Kress, M., H. E. Huxley, A. R. Faruqi, and J. Hendrix. 1986. Structural changes during activation of frog muscle studied by time-resolved x-ray diffraction. *J. Mol. Biol.* 188:325–342.

Luther, P. K., and J. M. Squire. 1980. Three-dimensional structure of the vertebrate muscle A-band II: the myosin filament superlattice. *J. Mol. Biol.* 141:409–439.

Lymn, R. W. 1978. Myosin sub-fragment-1 attachment to actin: expected effect on equatorial reflections. *Biophys. J.* 21:93–98.

Matsubara, I., N. Yagi, H. Miura, M. Ozeki, and T. Izumi. 1984. Intensification of the 5.9-nm actin layer line in contracting muscle. *Nature (Lond.).* 312:471–473.

Matsuda, T., and R. J. Podolsky. 1984. X-ray evidence for two structural states of the actomyosin cross-bridge in muscle fibers. *Proc. Natl. Acad. Sci. USA.* 81:2364–2368.

Miller, A., and R. T. Tregear. 1972. Structure of insect fibrillar flight muscle in the presence and absence of ATP. *J. Mol. Biol.* 70:85–104.

Nagano, H., and T. Yanagida. 1984. Predominant attached state of myosin cross-bridges during contraction and relaxation at low ionic strength. *J. Mol. Biol.* 177:769–785.

Parry, D. A. D., and J. M. Squire. 1973. The role of tropomyosin in muscle regulation: analysis of the x-ray diffraction patterns from relaxed and contracting muscles. *J. Mol. Biol.* 75:33–55.

Reedy, M. K., K. C. Holmes, and R. T. Tregear. 1965. Induced changes in orientation of the cross-bridges of glycerinated insect flight muscle. *Nature (Lond.).* 207:1276–1280.

Squire, J. M. 1990. Molecular Mechanisms in Muscular Contraction. MacMillan Press, Basingstoke, UK.

Squire, J. M. 1981. The Structural Basis of Muscular Contraction. Plenum Publishing Corp., New York.

Squire, J. M. 1988. Invisible actin makes its debut. *Nature (Lond.).* 335:590–591.

Squire, J. M., and J. J. Harford. 1988. Actin filament organisation and myosin head labelling patterns in vertebrate skeletal muscles in the rigor and weak-binding states. *J. Muscle Res. Cell Motil.* 9:344–358.

Stein, R., R. D. Ludescher, P. S. Dahlberg, P. G. Fajer, R. L. H. Bennett, and D. D. Thomas. 1991. Time-resolved rotational dynamics of phosphorescent-labeled myosin heads in contracting muscle fibres. *Biochemistry.* 29:10023–10031.

Vibert, P. J. 1988. Domain structure of the myosin head in correlation-averaged images of shadowed molecules. *J. Muscle Res. Cell Motil.* 9:147–155.

Wakabayashi, K., H. Tanaka, H. Saito, N. Moriwaki, Y. Ueno, and Y. Amemiya. 1991. Dynamic x-ray diffraction of skeletal muscle contraction: structural change of actin filaments. *Adv. Biophys.* 27:3–13.

Wakabayashi, K., Ueno, Y., Amemiya, Y., and H. Tanaka. 1988. Intensity changes of the actin-based layer-lines from frog skeletal muscles during an isometric contraction. *In* Molecular Mechanisms of Muscle Contraction. H. Sugi and G. H. Pollack, editors. Plenum Publishing Corp., London. 353–367.

Xu, S., M. Kress, and H. E. Huxley. 1987. X-ray diffraction studies of the structural state of crossbridges in skinned frog sartorius muscle at low ionic strength. *J. Muscle Res. Cell Motil.* 8:39–54.

Yagi, N. 1991. Intensification of the first actin layer-line during contraction of frog skeletal muscle. *Adv. Biophys.* 27:35–43.

Yagi, N., and I. Matsubara. 1989. Structural changes in the thin filament during activation studied by x-ray diffraction of highly stretched skeletal muscle. *J. Mol. Biol.* 208:359–363.

Yu, L. C. 1989. Analysis of equatorial x-ray diffraction patterns from skeletal muscle. *Biophys. J.* 55:433–440.

Yu, L. C., and B. Brenner. 1989. Structures of actomyosin cross-bridges in relaxed and rigor muscle fibers. *Biophys. J.* 55:441–453.

Yu, L. C., R. W. Lymn, and R. J. Podolsky. 1977. Characterization of a non-indexible equatorial x-ray reflection from frog sartorius muscle. *J. Mol. Biol.* 115:455–464.

Yu, L. C., A. C. Steven, G. R. S. Naylor, R. C. Gamble, and R. J. Podolsky. 1985. Distribution of mass in relaxed frog skeletal muscle and its redistribution upon activation. *Biophys. J.* 47:311–321.